Supporting Information to:

Fluorescence-based high throughput screening for noble metal-free and platinum-poor anode catalysts for the direct methanol fuel cell (DMFC)

F. G. Welsch, K. Stöwe, W. F. Maier*
Lehrstuhl für Technische Chemie, Universität des Saarlandes, Gebäude C4 2, 66123 Saarbrücken, Germany
* Corresponding author: Tel.: +496 81 302 2422
E-Mail address: w.f.maier@mx.uni-saarland.de

Serval diagrams and schemes are provided for more detailed understanding of the arguments and conclusions presented.

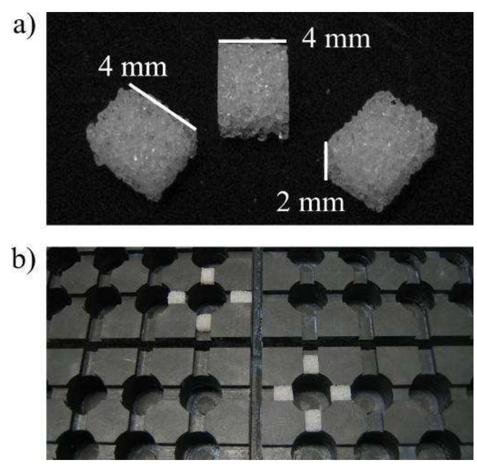

Fig. S1

Frits used for conventional measurements (a); frits positioned in the surrounding channels of the graphite plate relief (b).

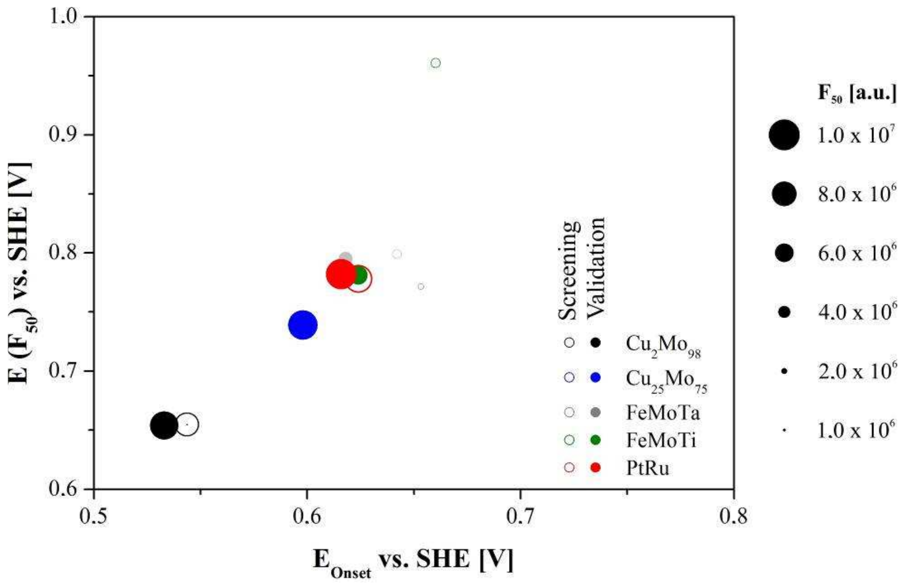

Fig. S2

Comparison of the noble-metal free materials´ activity towards the electrooxidation of methanol obtained in the high-throughput screening by means of their position in the $E(F_{50})/E_{Onset}$ plane and the fluorescence intensity F_{50}, cycles: position based on the comparative values determined in the high-throughput screening, filled cycles: position based on the comparative values determined in the fluorescence based validation measurements.

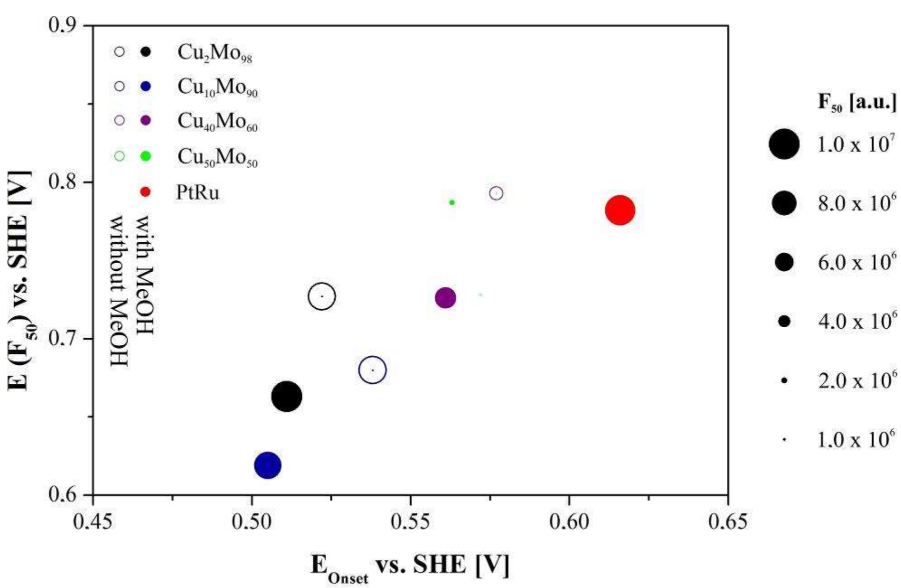

Fig. S3

Comparison of the fluorescence development of the compounds of the binary Cu-Mo system among the measurement with and without a methanol containing electrolyte by means of their position in the $E(F_{50})/E_{Onset}$ plane and the fluorescence intensity F_{50}; cycles: measurement without methanol, filled cycles: measurement with methanol.

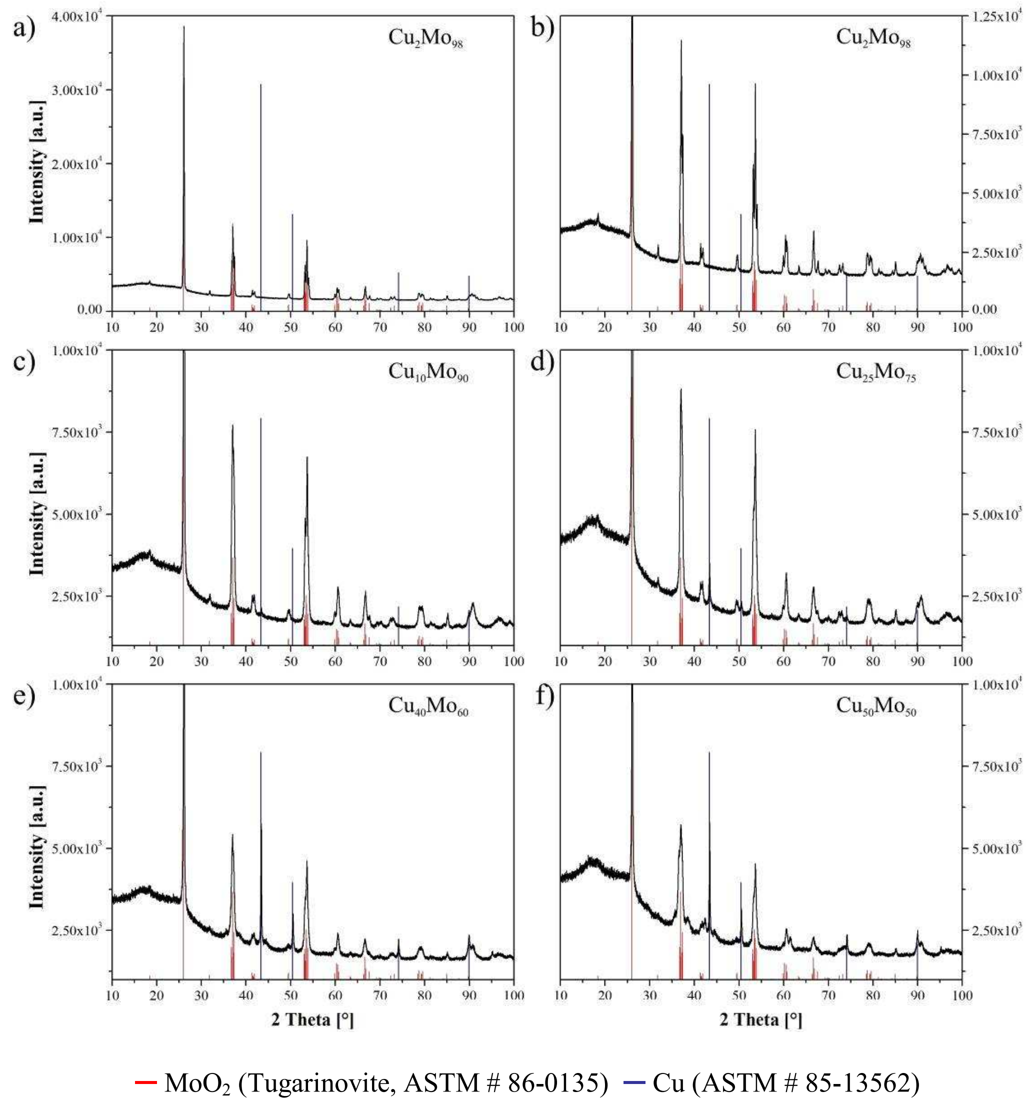

Fig. S4

X-ray diffraction pattern of a) Cu_2Mo_{98} (overview), b) Cu_2Mo_{98} (increased intensity scale), c) $Cu_{10}Mo_{90}$, d) $Cu_{25}Mo_{75}$, e) $Cu_{40}Mo_{60}$, f) $Cu_{50}Mo_{50}$; axis caption line by line and column by column, respectively.

Fig. S5

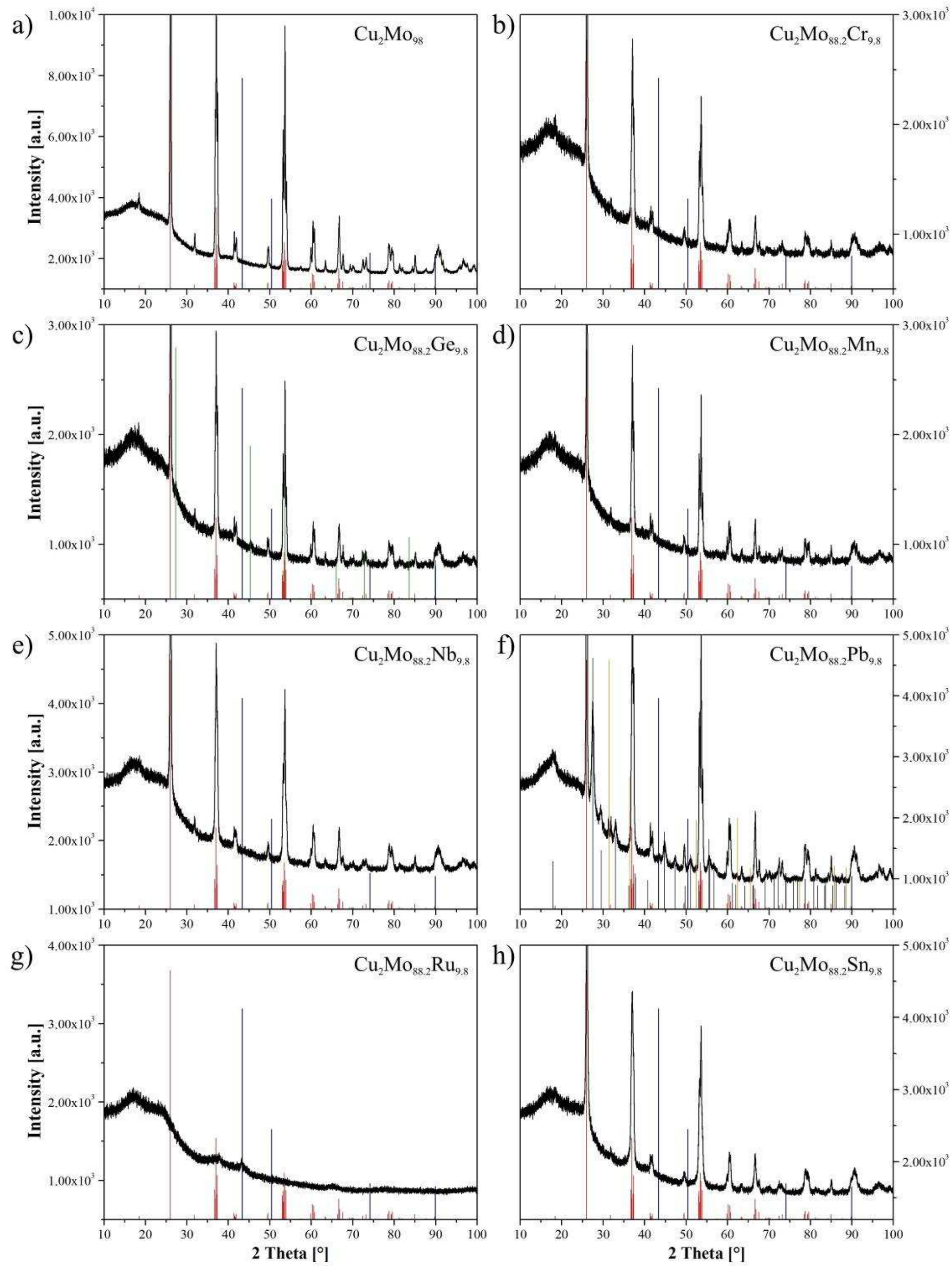

— MoO_2 (Tugarinovite, ASTM # 86-0135) — Cu (ASTM # 85-13562)

— Ge (ASTM # 4-545) — Pb (ASTM # 87-663) — $PbMoO_4$ (Wulfenite, ASTM # 74-1075)

Fig. S5

Powder X-ray diffraction pattern of a) Cu_2Mo_{98}, b) $Cu_2Mo_{88.2}Cr_{9.8}$, c) $Cu_2Mo_{88.2}Ge_{9.8}$, d) $Cu_2Mo_{88.2}Mn_{9.8}$, e) $Cu_2Mo_{88.2}Nb_{9.8}$, f) $Cu_2Mo_{88.2}Pb_{9.8}$, g) $Cu_2Mo_{88.2}Ru_{9.8}$, h) $Cu_2Mo_{88.2}Sn_{9.8}$; axis caption line by line and column by column, respectively.

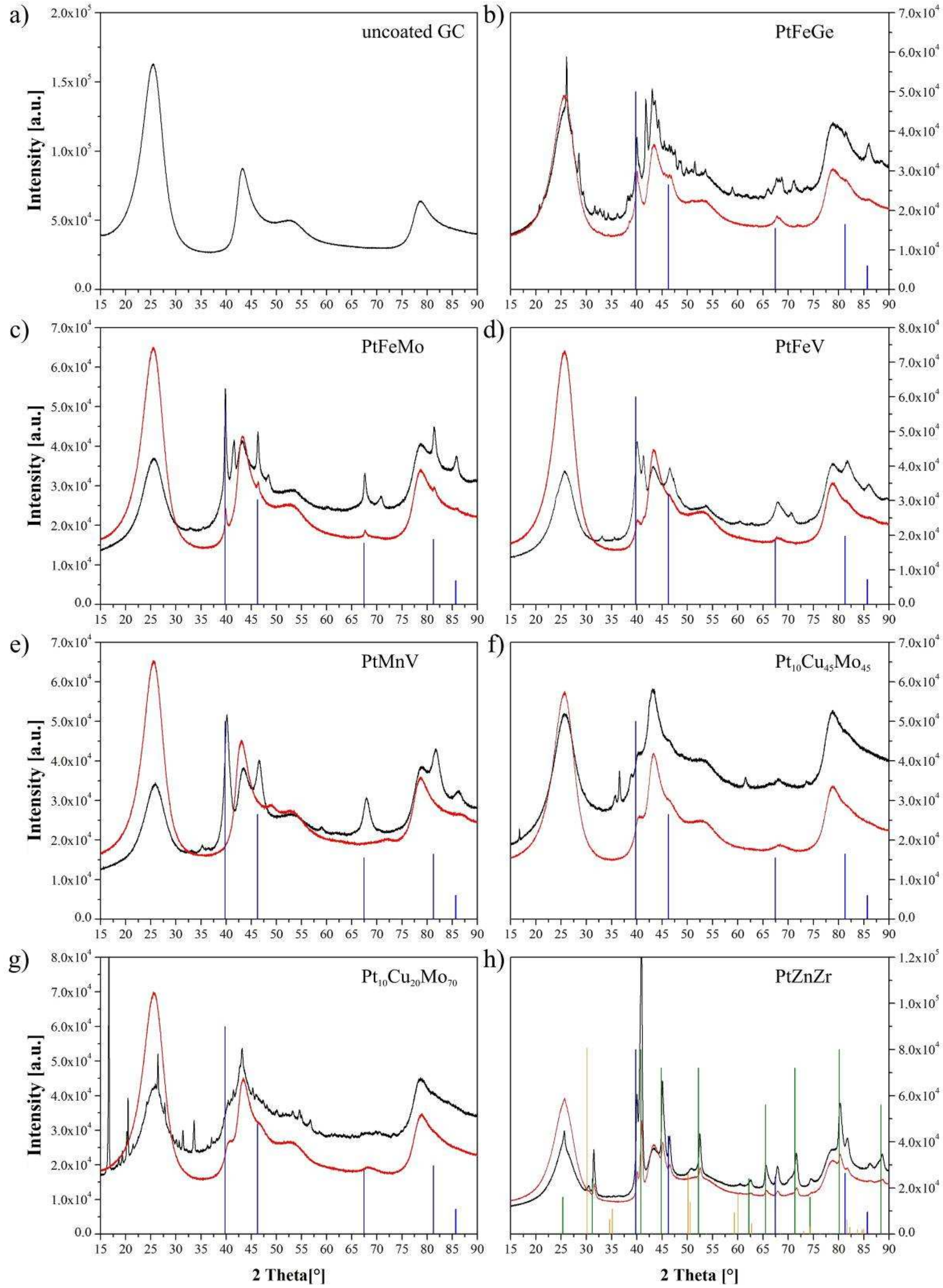

— Pt (ASTM # 04-0802) — PtZn (ASTM # 06-0604) — ZrO_2 (tetragonal, ASTM # 78-1601)

Fig. S6: X-ray diffraction pattern of a) uncoated glassy carbon plate, b) PtFeGe, c) PtFeMo, d) PtMnV, e) PtMnV, f) $Pt_{10}Cu_{45}Mo_{45}$, g) $Pt_{10}Cu_{20}Mo_{70}$ h) PtZnZr before (black) and after the CV experiments (red), reference line pattern were given only for identified phases after the stability experiments.